JAAS

Accepted Manuscript

ROYAL SOCIETY
OF CHEMISTRY

www.rsc.org/jaas

Determination of ^{129}I in Arctic snow by a novel analytical approach using IC-ICP-SFMS

Žilvinas Ežerinskis[1*], Andrea Spolaor[2,3], Torben Kirchgeorg[2], Giulio Cozzi[3], Paul Vallelonga[4], Helle A. Kjær[4], Justina Šapolaitė[1], Carlo Barbante[2,3], Rūta Druteikienė[1]

[1]State Research Institute, Center for Physical Sciences and Technology, Savanorių ave. 231, LT-02300 Vilnius, Lithuania

[2]Department of Environmental Sciences, Informatics and Statistics, Ca'Foscari University of Venice, Dorsoduro 2137, 30123, Italy

[3]Institute for the Dynamics of Environmental Processes-CNR, Venice, 30123, Italy

[4]Centre for Ice and Climate, Niels Bohr Institute, Juliane Maries Vej 30, 2100 Copenhagen, Denmark

Keywords: Iodine-129, Speciation analysis, sub-picogram per gram range, Fukushima, Arctic, NEEM, Greenland

Submitted to JAAS

Corresponding Author: zilvinas.ezerinskis@ftmc.lt, Savanorių ave. 231, LT-02300 Vilnius, Lithuania.

Abstract

The environmental radiation background has increased in the last century due to human nuclear activities and in this context ^{129}I may be used to evaluate the anthropogenic contribution to global nuclear contamination. We present a fast and novel method for iodine-129 measurements. Coupling ion chromatography and inductively coupled plasma sector field mass spectrometry (IC-ICP-SFMS) allows the determination of iodine-129 at picogram-per-gram levels. The capability of the Dionex IONPAC® AS16 column to retain iodine species in the absence of NaOH has been used to pre-concentrate 5 mL samples. Although ^{129}I suffers from isobaric spectral interference due to ^{129}Xe, the IC-ICP-SFMS technique allows ^{129}I to be determined by removing all other isobaric interferences. Further, the ^{129}Xe interference is sufficiently small and stable to be treated as a background correction. This strategy permits the evaluation of ^{129}I speciation at sub-picogram per gram levels with a limit of detection (LOD) of 0.7 pg g^{-1}. Thus the range of possible applications of this technique is expanded to low-concentration environmental samples such as polar snow. Preliminary results obtained from Greenland (NEEM) snow pit samples confirm its applicability for environmental research.

1. Introduction

The behaviour and occurrence of iodine isotopes, and in particular radioactive iodine-129 (^{129}I, half-life ($t_{½}$) = 1.57x10^{7} y) in natural systems is widely studied. Due to extremely high solubility in water and rather high concentrations in many cases iodine is used as an oceanographic tracer for studying transport and exchange of water masses[1], as well as a useful environmental tracer for investigating geochemical cycling of stable iodine[2]. In water pollution monitoring ^{129}I is measured in aquatic plants[3–6]. ^{129}I is naturally produced in small quantities, due to the spontaneous fission of natural uranium as well as by cosmic ray spallation of trace levels of xenon in the atmosphere. Anthropogenic sources are primarily formation from the fission of uranium and plutonium in nuclear reactors[7]. The isotope ^{129}I is one of the main radionuclides of long-term medium waste (e. g. operational waste) and high activity radioactive waste (spent nuclear fuel) storage facilities, and can be released during nuclear accidents. On 11 March 2011 a nuclear disaster occurred in Fukushima Daiichi Nuclear Power Plant (FDNPP). Several studies have assessed the amount and distribution of radionuclides ^{129}I, ^{131}I, ^{137}Cs and ^{134}Cs released by the accident [7–101, 2]. Paatero et al.[7] investigated the distribution of radionuclides in the atmosphere of the Arctic region and determined that the radioactivity released from FDNPP reached Svalbard in the middle of spring. SILAM model[7] calculations show that greater deposition may have occurred in Greenland and especially in the Northwest. A SILAM model scenario shows concentrations above 3000 µBq m^{-3} for ^{131}I at the height of 1 km above sea level for late March 2011[7].

Few studies of ^{129}I have been reported due to the sub-pg g^{-1} concentrations of ^{129}I present in environmental samples. Neutron activation and accelerator mass spectrometry techniques reach detection limits in the range of 10^{-18} g g^{-1} which is sufficiently sensitive to determine ^{129}I but these instruments may be costly and slow to access [11–13]. In turn, beta, gamma and X-ray spectrometric methods are commonly used for ^{129}I measurements but suffer from interferences and shielding phenomena and may require a long counting time for samples with low activities. An alternative approach for ^{129}I measurements is to use inductively coupled plasma mass spectrometry (ICP-MS)[14–16] which is 1000 times more sensitive[17] than the aforementioned spectrometric methods.

The aim of this study is to develop a method combining ion chromatography (IC) and inductively coupled plasma sector field mass spectrometry (ICP-SFMS) for the determination of ^{129}I. Online preconcentration[18] allows the LOD to be decreased to low pg g^{-1} levels as well as discriminating between inorganic iodine species and reducing isobaric and molecular interferences (^{129}Xe, $^{89}Y^{40}Ar$, $^{115}In^{14}N$, $^{113}Cd^{16}O$, $^{97}Mo^{16}O_2^+$), hydride $^{127}IH_2$ formation and matrix effects. We apply this new analytical method to determine ^{129}I in six snow pit samples from the Arctic NEEM ice core drilling camp located in Northwest Greenland.

2. Materials and Method

2.1 Working and chemicals

All reagent solutions and samples were prepared in a particle-free laboratory. The laboratory consists of a series of over-pressured working spaces with air qualities ranging from class 10 to 100 (US Fed. Std 209E, equivalent to ISO 4 to 5) supplied by modular HEPA fan-filter units (Envirco, Sanford NC, USA). All solutions were prepared using ultrapure water (UPW, 18.2 MΩ, ELGA Pure Lab, Marlow, United Kingdom). NaOH eluent solution was automatically produced by an eluent generator (Dionex ICS 5000 EG, Thermo Scientific). The final NaOH eluent concentration was 35 mM. To test the memory effect and washout time of the ICP-SFMS eluents were prepared from Tetramethylammonium hydroxide (TMAOH) solution (25%) and suprapure nitric acid (HNO_3 65%) purchased from Merck.

Chromatographic data analysis software (Xcalibur, Thermo Scientific, Bremen, Germany) was used for peak integration.

2.2 Standard solutions

$^{127}I^-$ and $^{129}I^-$ standards were used to test the applicability of the method by dilution of stock solutions. $^{127}I^-$ standards were prepared by diluting 1000 mg L^{-1} stock IC standard solutions (TraceCERT® purity grade, Sigma-Aldrich, MO, USA) in UPW. $^{129}I^-$ standards were prepared from a stock solution of I-129 purchased from the PTB (Physikalisch Technische Bundesanstalt, Braunschweig, Germany). This standard presented a certified specific activity of 1.01 kBq/g ± 3% (154 µg g^{-1} ^{129}I). The concentrations of the prepared standards were: 0.9, 2.9, 4.5, 9.3, 25.3, 42.7 and 93.3 pg g^{-1}. No $^{129}IO_3^-$ impurities were detected in the ^{129}I standard.

2.3 Sample description and preparation

In 2012 surface snow samples were collected from a 2 m deep snow pit at the North Greenland Eemian ice drilling (NEEM) site (77.45° N; 51.06° W, 2480 m a.s.l.) covering the period 2010-2012. Model simulation of FDNPP[7] fallout and deposition suggests that the contamination due to the FDNPP disaster should have reached the Greenland ice sheet. The snow pit walls were firstly scraped with a polyethylene bar, to remove any sections that were potentially contaminated during the digging and glaciological measurements. Sampling was conducted by plunging 5 mL low-density polyethylene (LDPE) vials perpendicularly into the snow-pit wall. The sampling has been performed from the surface down to the bottom of the snow-pit, with a spatial resolution of 5 cm which is suitable for sub-seasonal resolution. The bottles were capped and packed in double LDPE bags. Samples were kept frozen during transport and storage, then melted at room temperature under a class 100 clean bench. The melted samples were combined to obtain six samples (as described in table 3) with sufficient volume for ^{129}I determination. After collection, the samples were protected from sunlight to avoid photoactivation of iodine.

3. Apparatus and procedure

Measurements were carried out on an ion chromatographic system (Dionex ICS 5000, Thermo Scientific, Waltham, US) coupled to an inductively coupled plasma sector field mass spectrometer (ELEMENT2 Thermo Scientific, Germany) equipped with Peltier-cooled spray chamber (ESI, Omaha, US). All parameters regarding the ICP-SFMS and the sample introduction system are shown in table 1. Since the interference of xenon remains the main problem we adopted an approach using IC-ICP-SFMS to identify and isolate the peak of the inorganic species of $^{129}I^-$ above the ^{129}Xe background.

The ion chromatographic system was equipped with an AS 16 anion exchange column (2 mm x 250 mm, Thermo Scientific) and in addition we used an AS 16 guard column (2 x 50 mm). It is known that the AS16 column can be used for the separation of anion species as well as for iodine species pre-concentration [18]. This is because the use of UPW as a carrier allows the column to have the capacity to retain anionic compounds, including ^{129}I in the form of Iodide (I^-) and Iodate (IO_3^-). In this context we injected a large sample volume of 5 mL to pre-concentrate ^{129}I on the column. Samples were injected with a 5 mL injection loop. Pre-cleaned 5 mL plastic syringes and a syringe pump (11 Plus, Harvard Apparatus, Holliston, MA, US) were used to fill the sample loop. A gradient program using UPW and NaOH was necessary to pre-concentrate ^{129}I. NaOH was generated by an eluent generator (Dionex ICS 5000 EG, Thermo Scientific) to avoid any external contamination.

In a first step $^{129}I^-$ was pre-concentrated on the column using only UPW (0 – 15 min) followed by the elution with 35 mM NaOH (15 – 30 min) and a final re-conditioning step (30 – 35 min, UPW). The flow speed was 0.35 mL min^{-1}. The NaOH was removed by a suppressor (ASRS 300, 2 mm, 50 mA, Thermo Scientific) before entering the MS source. The ion chromatographic system was controlled with Chromeleon 6.8 (Thermo Scientific).

4. Results and Discussion

4.1 Linearity, blanks, and detection limits

The method was validated by using external calibration curves of ^{129}I (in the form of iodide) in the range of concentrations between 1 to 100 pg g^{-1}. Calibration curves of ^{129}I had a correlation coefficient greater than 0.99 (figure 1a) and decreased to 0.97 when evaluating only the standards from 0.9 to 4.5 pg g^{-1} (figure 1b). Considering the environmental concentrations of ^{129}I in polar samples from Greenland (in soil samples concentrations are in the low pg g^{-1} range), care was taken to evaluate the procedural blanks. The estimation was achieved by 10 repeat analyses of UPW and the limit of detection was defined as 3 times the standard deviation of the procedural blank, calculated to be 0.7 pg g^{-1}. The detection limits obtained are lower than previous published methods using collision reaction cell (CRC-ICP-MS, 1.1 pg g^{-1})[19] but an order of magnitude higher than triple quadrupole ICP-MS in MS/MS mode (0.07 pg g^{-1}) [20]. Our approach requires a longer analysis time (35 min per sample) compared to direct injection measurements (3 min per sample) but this is required to ensure the removal of most spectral interferences on I^{129}. Although the volume introduced is 5 mL the proposed method offers low residual standard deviations (%RSD) with the advantage of discriminating between the different ^{129}I inorganic species and without requiring sample pre-treatment.

4.2 Recovery, accuracy, reproducibility and internal standard

No certified reference material is available for ^{129}I in a polar ice matrix[17] so we adopted the method of analysing melted Arctic samples spiked with different concentrations of ^{129}I in order to evaluate the accuracy and recovery of the technique. The concentrations tested ranged between 1 and 10 pg g^{-1} (Table 2). ^{129}I had a recovery of 80% at concentrations of 1 pg g^{-1} compared with 77% recovery at 10 pg g^{-1}. Similar recoveries for samples with ^{127}I concentrations below 10 pg g^{-1} were obtained by Spolaor et al.[18] using a 0.3 mL volume loop instead of a 5 mL. Considering that there are no standard procedures to calculate the ^{129}I recovery we use the external calibration equation obtained from UPW standard where we have a slope of 1967 area/pg g^{-1} and an intercept of 2500. We choose to proceed in this way because the matrix effect is minimized by the chromatographic ion suppressor that removes all cations from the ice matrix. Furthermore the different anions, including iodine, have different retention times thereby minimizing the possibility of competing ions in the plasma. The specifications of the Dionex AS16® column clearly show that the major anions present in polar snow (such as chloride and sulphate) are eluted faster than iodide. Therefore we can consider that the instrumental matrix effect is minimized and the most likely explanation for the decreased recovery of real samples is due to the efficiency of the chromatographic column. It is possible that the higher concentrations of ions such as chloride, sulphate and bromide could cause a lower retention of iodide by the column therefore decreasing the final recovery.

Reproducibility was evaluated by repeating three measurements for each individual standards (concentrations of tested standards were: 0.9, 2.9, 4.5, 25.1 and 42.7 pg g^{-1}). Results demonstrate low %RSDs between 10% to 2.5% for the lowest and highest concentrations of the standard solutions, respectively. Additionally the precision has been evaluated in a 10 pg g^{-1} $^{129}I^{-}$ spiked NEEM sample. The %RSD calculated is in the same range as the value obtained for the standard tested (5 %).

To ensure the quality of measurements and estimate matrix effects, the use of an internal standard is the most common method. The principle of the internal standard is that the analyte and the internal standard should have the same behaviour during all steps of the analyses. In the literature different internal standards have been used for iodine analysis: Te, Re and Cs [21,22]. The use of Cs as an internal standard is doubtful because of its different chemical and physical properties compared to iodine. Caesium is unsuitable not only due to its different behaviour in alkali solutions[6], but also because of its extremely low first ionization potential of 3.8 eV compared to iodine (10.4 eV)[22]. The first ionization potential of I appears on the slope of the curve which makes iodine sensitive to matrix effects whereas Cs is completely ionized and almost independent of concomitant elements in plasma[23]. The quite different mass of Re, compared to I, also limits its suitability as an internal standard. Tellurium would be more suitable because of its similar mass and ionization potential, but there is a risk of isobaric interferences arising from the formation of ^{128}TeH. Therefore internal standard was not used.

In the case of ICP-SFMS it xenon is present as a trace impurity in the argon carrier gas and hence cannot be easily reduced or eliminated. Consequently we have evaluated the stability of the xenon signal to evaluate if a reliable background-correction can be applied. Xenon isotopes ^{128}Xe, ^{131}Xe and ^{132}Xe were monitored to check argon gas during the various measurement sessions and furthermore we tested the xenon background level for 6 hours from one argon cylinder (50L, 200 bar, purity 99.996%). Results from this experiment showed that during the period of time usually required for a measurement (3 – 35 min) the xenon background was stable, with a precision of 15% (%RSD) for 0.01s sampling time and less than 5% for 0.05 s sampling time. The xenon signal was observed to be stable even when the tank was nearly empty.

Monitoring of xenon isotopes was also required to compensate for the presence of polyatomic interferences on ^{129}I, as described below.

4.3 Interferences of iodine hydride and polyatomic ions

Another problem of ^{129}I analysis by ICP-SFMS is $^{127}IH_2$ formation. This has to be taken into account, due to high abundance of ^{127}I in soil (around 2 μg g^{-1}) and marine systems[24]. Figure 2 depicts xenon isotope ratio changes based on the concentration of ^{127}I. In figure 2 (open squares) we can see that the ratio of the signal begins to increase at ^{127}I concentrations of approximately 100 ng g^{-1}. Thus as iodine concentrations increase, more IH is formed and eventually exceeds the ^{128}Xe background. This hypothesis was also tested for ^{129}Xe because of the potential for isobaric interference on ^{129}I [16]. Figure 2 shows that $^{127}IH_2$ (open circles) is not detectable below ^{127}I concentrations of 5000 ng g^{-1}.

Hydride formation strongly depends on the equipment used and its parameters, such as sample uptake rate, sample gas flow rate and plasma temperature, among others[25]. The parameters of the present work are given in table 1. According these estimates we can be sure that in this study hydride of iodine-127 does not interfere with our target analyte because the maximum abundance of ^{127}I in Greenland polar ice systems reaches 50-80 pg g^{-1} [26,27].

Polyatomic interferences such as $^{97}Mo^{16}O_2^+$, $^{115}In^{14}N^+$ *and* $^{113}Cd^{16}O^+$ can affect the signal of I^{129} especially for direct ICP-SFMS measurements. However an advantage of coupling ion chromatography with ICP-SFMS is the separation of Mo, In and Cd from ^{129}I. In polar samples, Mo, In and Cd are present at low pg g^{-1} concentrations however the capability of the resin to collect anions allows the separation of these elements from I^{129}. Additionally these elements in the free form are positively charged and can therefore be removed by the ion suppressor before entering the ICP-SFMS. Even if these elements are present in insoluble dust particles, the guard column should trap such particles before entering the analytical column or detector. Therefore, when the iodine is eluted from the column these interfering elements are not present.

On-line desolvation systems are often used to minimize interferences derived from oxide and hydride formation[28]. In this case one such system (Apex-Q, Elemental Scientific, USA) was tested. With the Apex-Q, we were able to increase the sensitivity of our target analyte by three times but at the same time we increased the background of xenon by ten times, because of the nitrogen carrier gas required by the system. Consequently, all ^{129}I measurements were carried out using a Cyclonic Peltier spray chamber due to its superior signal to noise ratio.

4.4 System washout and memory effects

Memory effects are an important issue to consider for the analysis of halogens and particularly iodine. To test this, we first evaluated the ICP-SFMS memory effect using a 50 ng g^{-1} ^{127}I standard solution by various approaches. An experiment was carried out as a single measurement using a continuous scanning mode. A washout solution of 2% HNO_3 for 5 minutes was sufficient to remove more than 99% of the iodine standard signal from the system. Ultra pure water (UPW) of pH 4.7-5.2 has a similar washout efficiency. An alkaline 1% tetramethylammonium hydroxide (TMAOH) solution was also tested but removed only 70% of iodine for the same washing procedure. The relatively low cleaning efficiency of alkaline solution may be due to the reactions that take place in the spray chamber. Larger droplets containing iodine may be deposited on the spray chamber walls and the alkaline solution fails to remove them, whereas deionized water may carry volatile iodine derivatives such as HI and I_2 with the nebulizer gas stream to the plasma. Iodine is extremely soluble in water. Such effects were observed in a previous study[29].

None of these memory effects were observed when the ICP-SFMS was coupled with IC using a carrier stream of UPW. Most of the matrix ions were removed by the IC, with anions retained on the column and cations removed by the suppressor. This combination ensured that deionized water was delivered to the ICP-SFMS. As the load process requires 15 minutes, the ICP-SFMS is effectively in “cleaning mode” for 15 minutes before each analysis. Considering only iodine, the instrument has a further 10 minutes of cleaning before the iodine is eluted from the column. Hence, the measurement cycle proposed here is effectively divided between 25 minutes of cleaning and 5 minutes of analysis, which is quite sufficient to ensure that any memory effect is sufficiently minimized. Peak tailing was observed for I concentrations above 10 pg g^{-1}, but this phenomena influences the shape of the peak rather than the memory effect or background level. Therefore, a memory/peak tailing effect could be present for concentration above 10 pg g^{-1}, but such concentrations are very unlikely in polar snow. Iodine isotopes were monitored continuously using online chromatogram software. As can be seen from Figure 3, a washing time of 5 minutes is quite sufficient to reach background levels using an ultrapure water eluent.

Consequently, we can be confident to exclude any possibility of memory effect between samples uding the techniques described here.

4.5 Greenland snow pit samples

To test the method we analysed six snow pit samples from NEEM site in Northwest Greenland. We choose this location for two reasons: first the preliminary results obtained by the project RAPID (Tracking Radioactive Fallout from the Fukushima Daiichi Disaster in Arctic Snow) [30] clearly show a ^{137}Cs signal in two locations in Greenland (Barrel site, 76°93' N, 63°12' W, 1685 m a.s.l. and Summit Station, 72°58' N, 38°45' W, 3200 m a.s.l.) originating from the Fukushima Daiichi nuclear reactor incident. The second reason results from the findings of Paatero et al.[7], whose model calculations suggest an ^{131}I activity concentration of up to 3000 μBq m^{-3} at a height of 1 km above Northern Greenland. The NEEM snow pit covers the past two years of snow deposition, from summer 2010 to summer 2012 (figure 4). Although samples were combined to provide sufficient volume for ^{129}I analysis, we were still able to discriminate summer and winter 2010; summer, spring and winter 2011 and spring 2012 (6 samples, Table 3). The combined samples were analysed directly without any handling or pre-treatment. Samples covering spring 2012, summer 2010 and 2011, and winter 2010 and 2011 presented values in the blank range (close to 2600 integrated area). The sample corresponding to spring 2011 showed a signal (figure 4) with an integrated area of 4650, more than three standard deviations above the blank. Even though the signal was close to the detection limit, the chromatogram peak was clearly evident and allowed an ^{129}I concentration of 1.2 ± 0.2 pg g^{-1} to be determined. We can exclude the possibility of external contamination, artefacts or retention time changes in the sample for the following reasons: a) the method has been shown to be free from any memory effects; b) if the signal were due to ^{129}Xe, changes should have also been observed for ^{131}Xe and ^{132}Xe but this was not the case; c) no contamination from the laboratory environment was detected in the lower standard over the 10 days period corresponding to the measurement period; d) the retention time of ^{129}I is the same as that of ^{127}I (figure 5) thereby excluding the possibility of a random background fluctuation of ^{129}I at the time of elution ; e) The constant ^{131}Xe and ^{132}Xe signals also exclude the possibility of ^{127}I hydride formation (figure 2). The ^{129}I signal corresponds to the same deposition time as the ^{137}Cs signal determined by the RAPID project (figure 4). These results suggest the occurrence and deposition of ^{129}I at the NEEM site originating from the Fukushima Daiichi nuclear reactor incident.

Though other sources must be considered, such as La Hauge and Sellafield for north Europe contamination as propose from other authors[3, 4], the main contributions for north Greenland deposition are originated from Asia and North America [31]. Several studies have investigated the origin of air masses and deposition on the Greenland ice sheet by using isotopic [32] and back trajectory [33] approaches and identified, Asia and North America as the main sources of dust and air masses and confirming a marginal role of the air mass coming from the Europe. These findings are also confirmed by a recent study investigating the source of biomass burning compounds in NEEM ice core where Asia, North America and Siberia were identified as the main sources [34]. Only a few European volcano layers were detected in the volcanism history from the NEEM ice core [35].

In additions if a contamination was due a continuously emission we should be able to detect ^{129}I signal in all our samples instead in just one in corresponded of the Fukushima disaster. Thought a south to north atmospheric transport is very unlikely but not impossible from Europe to Greenland, we cannot totally exclude that these reprocessing plant could have no contribution to the contaminations, but we can suggest that this signal was most likely due to the Fukushima accident. In sustain to our hypothesis the presence of ^{134}Cs and ^{137}Cs in adjacent Greenland locations during spring 2011 strengthens our finding suggesting that the Fukushima disaster had an impact on remote regions of the North Hemisphere such as Greenland.

5. Conclusions

We present a method for the determination of ^{129}I with sub-picogram per gram detection limits and apply the technique to snow pit samples from northwest Greenland. The proposed method is fast and economical compared to AMS and neutron activation techniques as it requires neither sample preconcentration nor access to specialized accelerator facilities. The detection limit has been calculated as 0.7 pg g^{-1} with a precision of better than 90%. The recovery of the method is 72% for concentrations close to the detection limit but increases to 81% for concentrations above 1 pg g^{-1}. Although the injected sample volume was 5 mL, no memory effect was detected and the accuracy of the technique is comparable to results reported for 0.3 mL injection volumes[20]. The precision obtained here is less than the method reported for ^{127}I but this is due to the presence of Xe-129 which increases the background noise level.

The method was developed for snow samples or similar clean matrices and has been employed to investigate possible radioactive contamination of remote locations such as the Arctic. Testing this in Greenland snow pit samples, our results confirm the deposition of radioactive compounds emitted from the Fukushima Daiichi nuclear reactor incident on 11 March 2011. We found ^{129}I (1.2 pg g^{-1}) above detection limits (0.7 pg g^{-1}) in one of six snow samples analysed, covering the period of early spring of 2011. This approach could be a starting point for investigation of harmful radioactive elements in other glaciated regions such as the Himalayas, Andes and Alps, which are a source of potable water to large, densely-populated areas.

Acknowledgements

This project was funded by European Union Structural Funds project ”Postdoctoral Fellowship Implementation in Lithuania” within the framework of the Measure for Enhancing Mobility of Scholars and Other Researchers and the Promotion of Student Research (VP1-3.1-ŠMM-01) of the Program of Human Resources Development Action Plan.

In addition we would like to thank Elga Lab water, High Wycombe, UK, for supplying the pure water systems used in this study. We would also like to thank the three anonymous reviewers for their valuable comments which help us to improve the manuscript.

References

1. P. H. Santschi and K. a Schwehr, *Sci. Total Environ.*, 2004, **321**, 257–71.
2. X. Hou, *J. Radioanal. Nucl. Chem.*, 2004, **262**, 67–75.
3. G. M. Raisbeck and F. Yiou, *Sci. Total Environ.*, 1999, **237-238**, 31–41.
4. S. M. Keogh, a. Aldahan, G. Possnert, L. L. Vintró, P. I. Mitchell, K. J. Smith, and P. McGinnity, *Nucl. Instruments Methods Phys. Res. Sect. B Beam Interact. with Mater. Atoms*, 2010, **268**, 1232–1235.
5. S. Persson, a. Aldahan, G. Possnert, V. Alfimov, and X. Hou, *Nucl. Instruments Methods Phys. Res. Sect. B Beam Interact. with Mater. Atoms*, 2007, **259**, 508–512.

6. J. Zheng, H. Takata, K. Tagami, T. Aono, K. Fujita, and S. Uchida, *Microchem. J.*, 2012, **100**, 42–47.

7. J. Paatero, J. Vira, M. Siitari-Kauppi, J. Hatakka, K. Holmén, and Y. Viisanen, *J. Environ. Radioact.*, 2012, **114**, 41–47.

8. S. Otosaka, K. A. Schwehr, D. I. Kaplan, K. A. Roberts, S. Zhang, C. Xu, H.-P. Li, Y.-F. Ho, R. Brinkmeyer, C. M. Yeager, and P. H. Santschi, *Sci. Total Environ.*, 2011, **409**, 3857–3865.

9. X. Hou, P. P. Povinec, L. Zhang, K. Shi, D. Biddulph, C.-C. Chang, Y. Fan, R. Golser, Y. Hou, M. Ješkovský, a J. T. Jull, Q. Liu, M. Luo, P. Steier, and W. Zhou, *Environ. Sci. Technol.*, 2013, **47**, 3091–8.

10. S. C. Liu, C.-A. Huh, F.-J. Lin, C.-Y. Chan, S.-H. Lin, and S.-C. Hsu, *Geophys. Res. Lett.*, 2012, 39.

11. E. Robens and D. C. Aumann, *J. Environ. Radioact.*, 1988, **7**, 159–175.

12. X. Hou, H. Dahlgaard, B. Rietz, U. Jacobsen, S. P. Nielsen, and A. Aarkrog, *Analyst*, 1999, **124**, 1109–1114.

13. F. P. Brauer, Conference: 11. annual DOE low level waste management conference, Pittsburgh, PA, USA, 22-24 Aug 1989;

14. R. J. Cox, C. J. Pickford, and M. Thompson, *J. Anal. At. Spectrom.*, 1992, **7**, 635–640.

15. O. T. Farmer, C. J. Barinaga, and D. W. Koppenaal, *J. Radioanal. Nucl. Chem.*, 1998, **234**, 153–157.

16. P. Bienvenu, E. Brochard, E. Excoffier, and M. Piccione, *Can. J. Anal. Sci. Spectrosc.*, 2004, **49**, 423–428.

17. X. Hou and P. Roos, *Anal. Chim. Acta*, 2008, **608**, 105–39.

18. A. Spolaor, P. Vallelonga, J. Gabrieli, N. Kehrwald, C. Turetta, G. Cozzi, L. Poto, J. M. C. Plane, C. Boutron, and C. Barbante, *Anal. Bioanal. Chem.*, 2013, **405**, 647–54.

19. Y. Shikamori, N. Sugiyama, and S. Kakuta, *Agil. Technol. Appl. note*, 2012.

20. T. Ohno, Y. Muramatsu, Y. Shikamori, C. Toyama, N. Okabe, and H. Matsuzaki, *J. Anal. At. Spectrom.*, 2013, **28**, 1283.

21. Y. Muramatsu, Y. Takada, H. Matsuzaki, and S. Yoshida, *Quat. Geochronol.*, 2008, **3**, 291–297.

22. H. Yamada, T. Kiriyama, and K. Yonebayashi, *Soil Sci. Plant Nutr.*, 2012, 37–41.

23. P. Serapinas, J. Šalkauskas, Ž. Ežerinskis, and A. Acus, *Spectrochim. Acta Part B At. Spectrosc.*, 2010, **65**, 15–23.

24. L. Y. Zhang and X. L. Hou, *Radiochim. Acta*, 2013, **540**, 130729000243004.

25. J. A. C. Broekaert, *Analytical Atomic Spectrometry with Flames and Plasmas*, Wiley-VCH, 2005.

26. A. Spolaor, P. Vallelonga, J. M. C. Plane, N. Kehrwald, J. Gabrieli, C. Varin, C. Turetta, G. Cozzi, R. Kumar, C. Boutron, and C. Barbante, *Atmos. Chem. Phys.*, 2013, **13**, 6623–6635.

27. A. Spolaor, J. Gabrieli, T. Martma, J. Kohler, M. B. Björkman, E. Isaksson, C. Varin, P. Vallelonga, J. M. C. Plane, and C. Barbante, *Cryosph.*, 2013, **7**, 1645–1658.

28. *Mass Spectrometry Handbook*, John Wiley & Sons, 2012.

29. F. Hans Vanhoe and Allemeersch, *Analyst*, 1993, **118**, 1015–1019.

30. *Proj. RAPID Track. Radioact. Fallout from Fukushima Dai-ichi Disaster Arct. Snow*.

31. F. E. Bory, A. J. M., Biscaye, P. E. and Groussett, *Geophys. Res. Lett.*, **30**, 16–1 – 16–4.

32. M. Lupker, S. M. Aciego, B. Bourdon, J. Schwander, and T. F. Stocker, *Earth Planet. Sci. Lett.*, 2010, **295**, 277–286.

33. D. W. Kahl, A. Martinez, I. Davidson, M. Harris, and O. Ax, *J. Geophys. Res.*, 1997, **102**, 26,861–26,875.

34. P. Zennaro, N. Kehrwald, J. R. Mcconnell, S. Schüpbach, and O. Maselli, *Clim. Past*, 2014, 809–857.

35. Michael Sigl, J. R. McConnell, L. Layman, O. Maselli, D. Pasteris, K. McGwire, D. Dahl-Jensen, J. P. Steffensen, B. M. Vinther, R. Edwards, R. Mulvaney, and S. Kipfstuhl, *J. Geophys. Res.*, 2012, **118**, 1151–1169.

FIGURES

Figure 1. External calibration curve of iodine-129 a) for standard concentrations between 0.9 and 97 pg g^{-1} b) considering standard concentrations between 0.9 and 4.5 pgg^{-1}

Figure 2^{127}IH and ^{127}IH$_2$ hydride formation graph. Squares indicate ^{127}IH hydride formation as the ^{128}Xe/^{131}Xe isotope ratio changes with ^{127}I concentration and circles show ^{127}IH$_2$ hydride formation as the ^{129}Xe/^{131}Xe isotope ratio changes with ^{127}I concentration.

Figure 3. Chromatogram of an ^{127}I$^-$ and ^{129}I$^-$ standard. The signal shows that after the first elution the background value is reached again in approximately 5 minutes.

Figure 4. Comparison between the ^{129}I$^-$ signal detected in the Greenland NEEM snow pit with ^{137}Cs signals at two other Greenland locations (Barrel site, 76°93' N, 63°12' W, 1685 m a.s.l. and Summit Station, 72°58' N, 38°45' W, 3200 m a.s.l.). Squares, triangles and circles show the δ^{18}O values indicating seasonality. Less-negative δ^{18}O values (shaded vertical bars) correspond to summer temperature maxima and more-negative δ^{18}O values correspond to winter temperature minima. Each horizontal bar corresponds to one sample. Dashed line correspond to the detection limit (D.L. of 0.7 pg g^{-1}) of the method proposed.

Figure 5. Chromatogram of the NEEM snow pit sample corresponding to spring 2011 (85 cm depth). Here ^{129}I and ^{127}I absolute signal intensities are plotted.

1 **Figure 1**

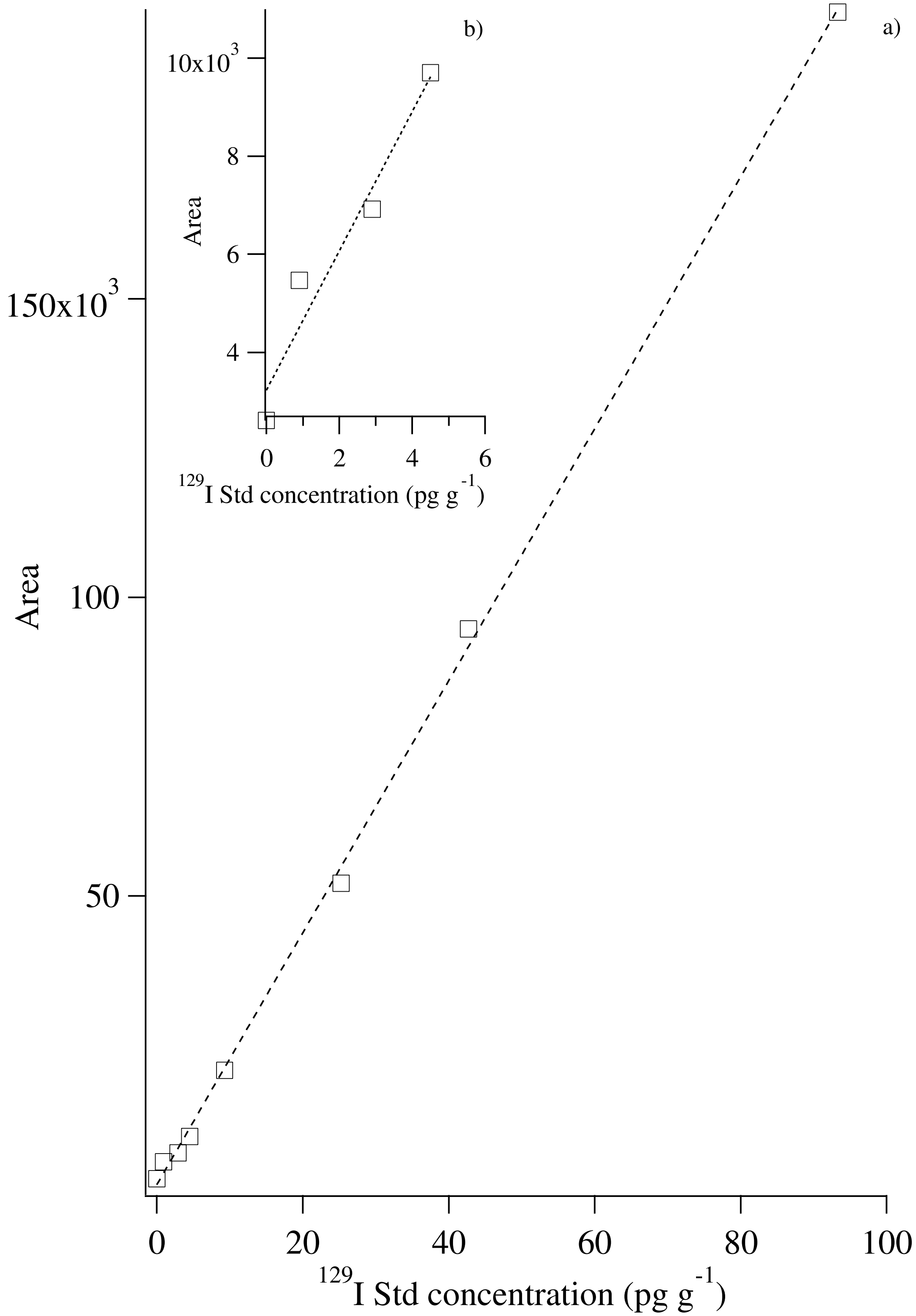
b)
a)
10x10^3
8
6
4
Area
0
2
4
6
129I Std concentration (pg g-1)
150x10^3
100
50
Area
0
20
40
60
80
100
129I Std concentration (pg g-1)

2

1 **Figure 2**

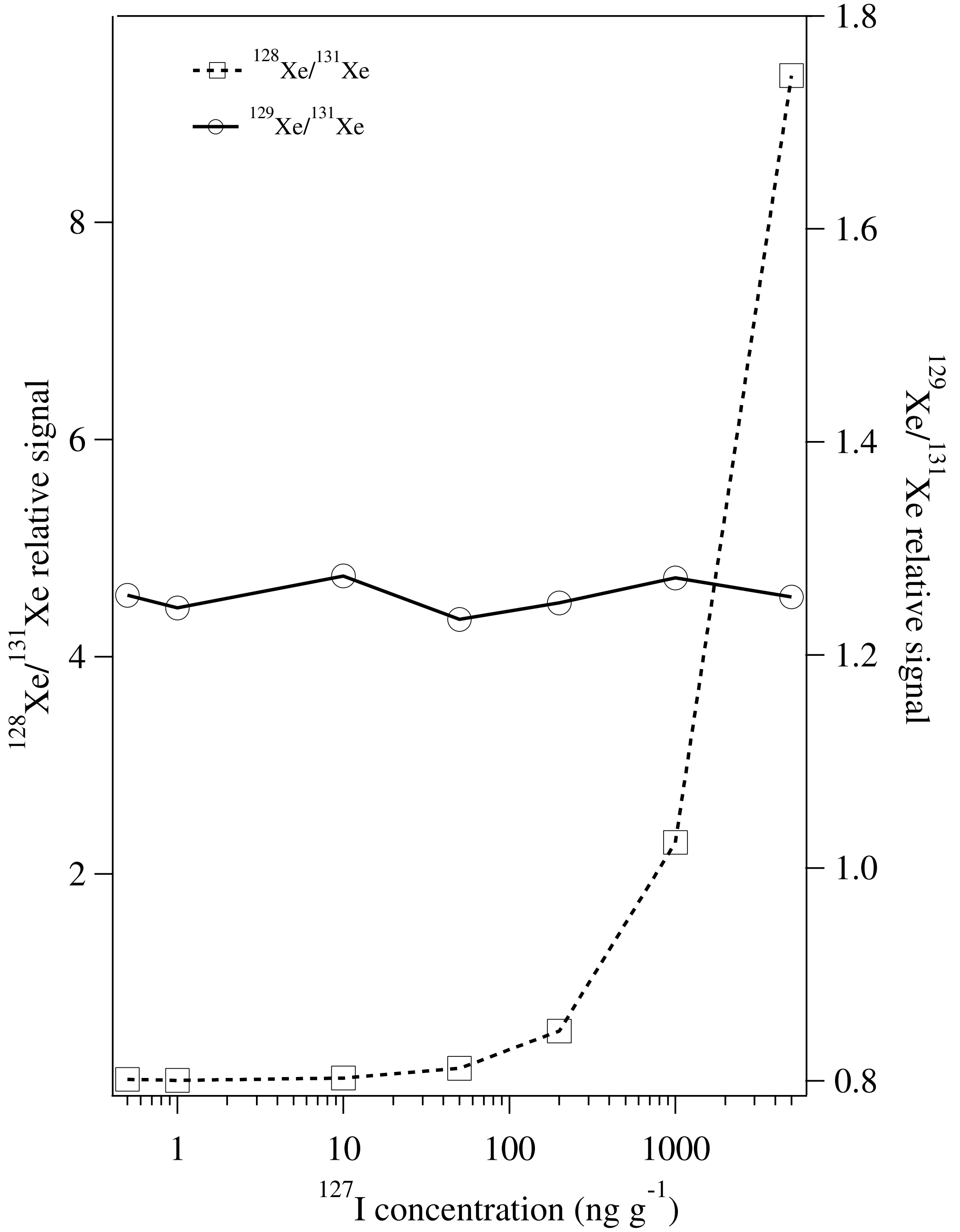

^{128}Xe/^{131}Xe
^{129}Xe/^{131}Xe
^{128}Xe/^{131}Xe relative signal
^{129}Xe/^{131}Xe relative signal
^{127}I concentration (ng g^{-1})
2
4
6
8
0.8
1.0
1.2
1.4
1.6
1.8
1
10
100
1000

2

3

Figure 3

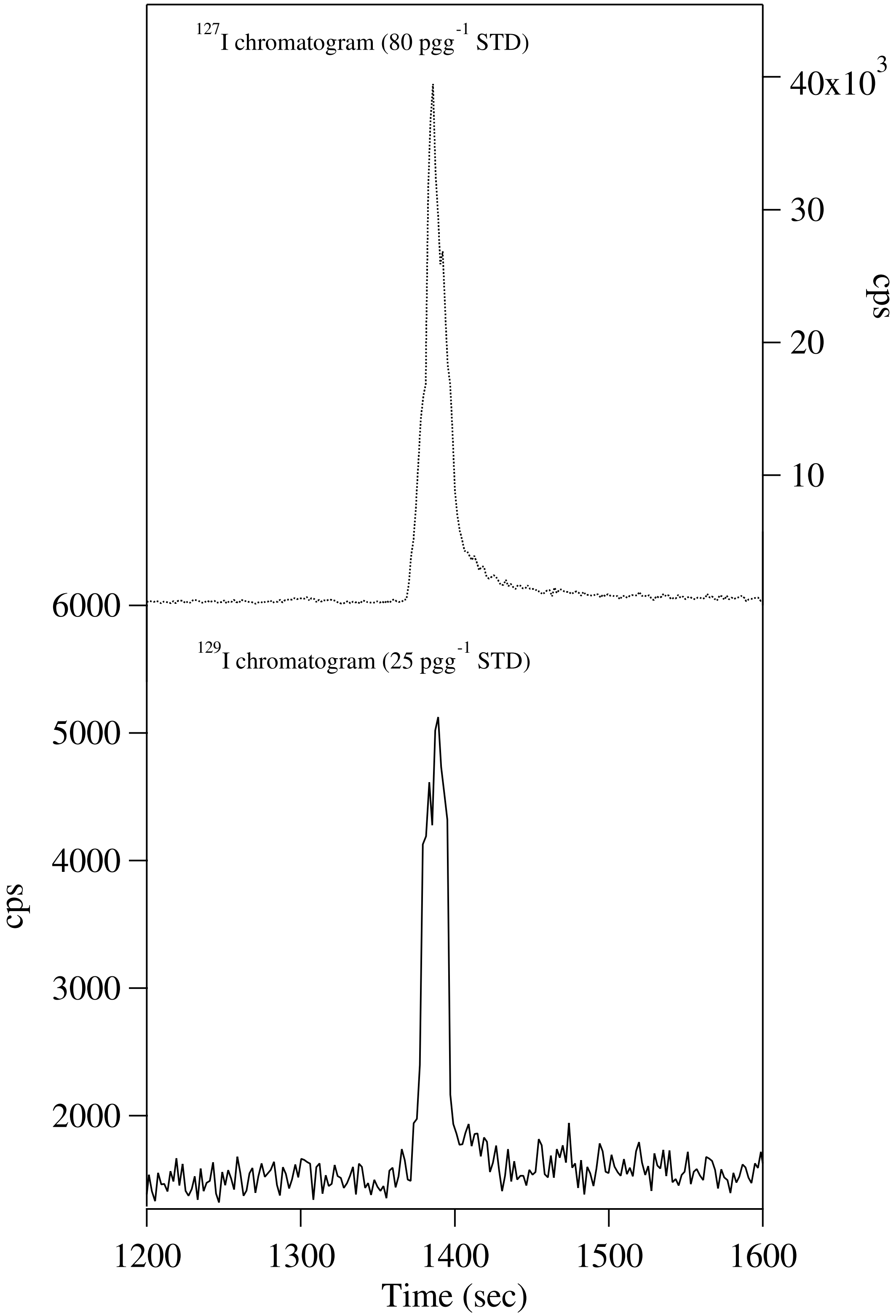
^{127}I chromatogram (80 pgg^{-1} STD)
40x10^3
30
20
10
cps
^{129}I chromatogram (25 pgg^{-1} STD)
6000
5000
4000
3000
2000
cps
1200
1300
1400
1500
1600
Time (sec)

Figure 4.

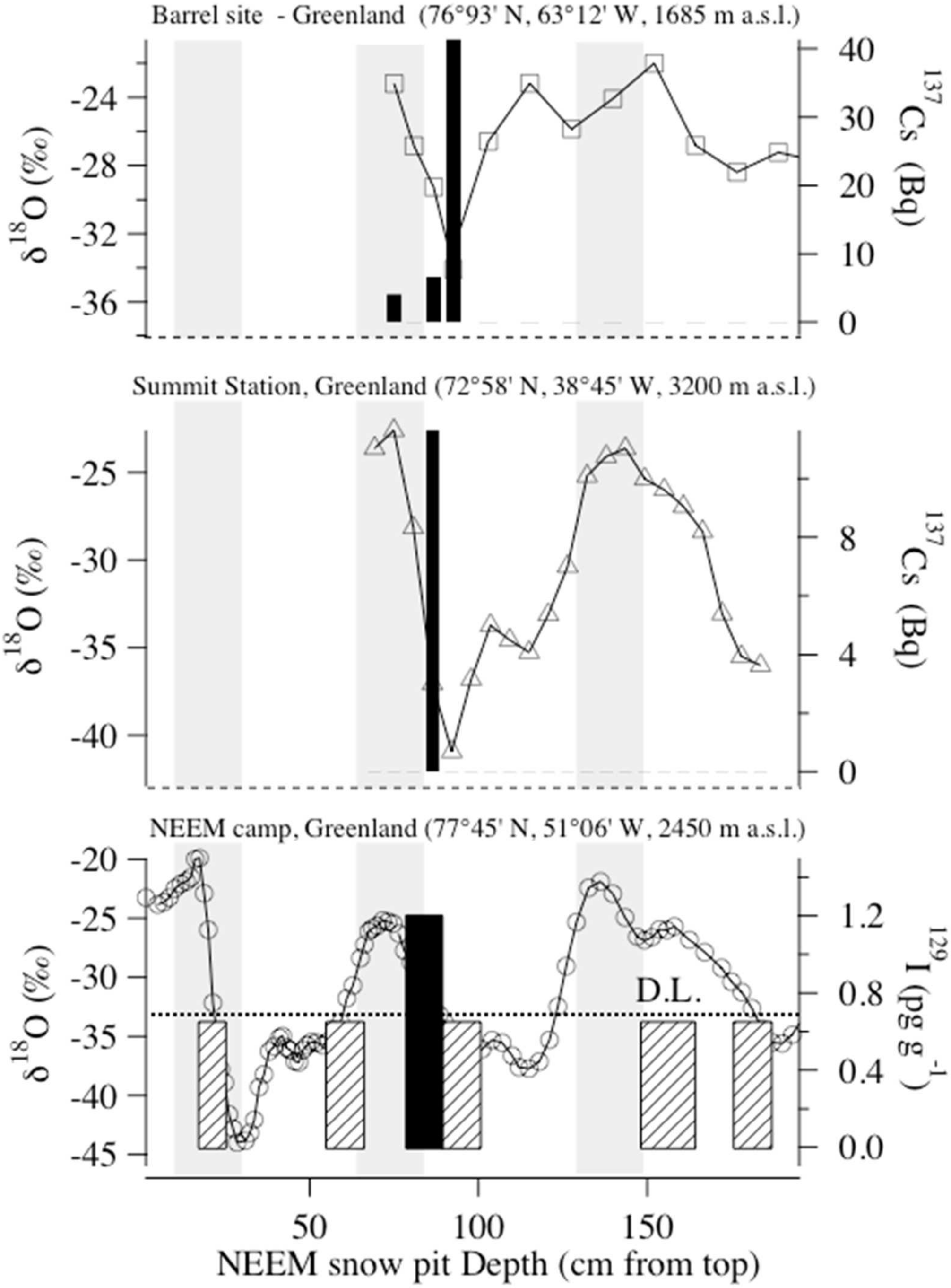
Barrel site - Greenland (76°93' N, 63°12' W, 1685 m a.s.l.)
δ^{18}O (‰)
-24
-28
-32
-36
^{137}Cs (Bq)
40
30
20
10
0
Summit Station, Greenland (72°58' N, 38°45' W, 3200 m a.s.l.)
δ^{18}O (‰)
-25
-30
-35
-40
^{137}Cs (Bq)
8
4
0
NEEM camp, Greenland (77°45' N, 51°06' W, 2450 m a.s.l.)
δ^{18}O (‰)
-20
-25
-30
-35
-40
-45
^{129}I (pg g^{-1})
1.2
0.8
0.4
0.0
D.L.
50
100
150
NEEM snow pit Depth (cm from top)

Figure 5

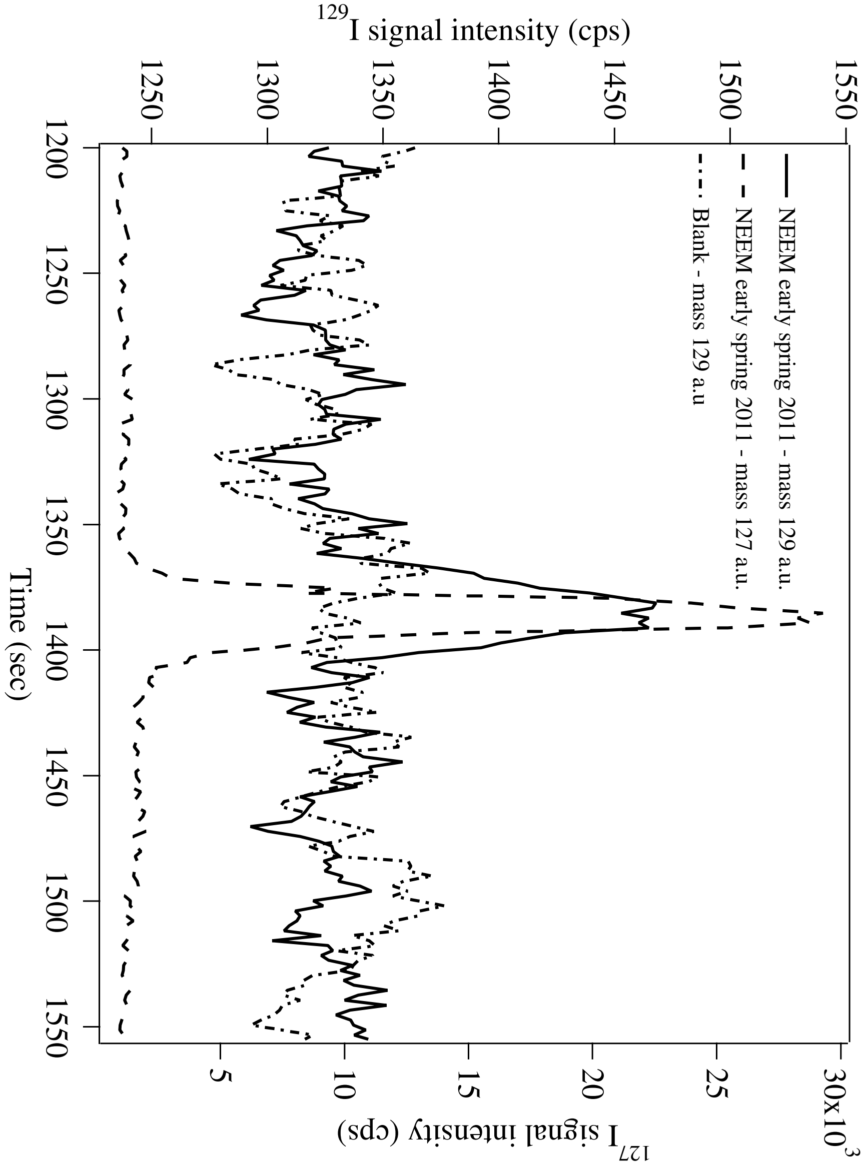
NEEM early spring 2011 - mass 129 a.u.
NEEM early spring 2011 - mass 127 a.u.
Blank - mass 129 a.u
^{129}I signal intensity (cps)
1250
1300
1350
1400
1450
1500
1550
Time (sec)
1200
1250
1300
1350
1400
1450
1500
1550
^{127}I signal intensity (cps)
5
10
15
20
25
30x10^3

TABLES

Table 1. Instrumental parameters for IC-ICP-SFMS

ICP-SFMS		
	Plasma Power	1350 W
	Cool gas	16.00 L min^{-1}
	Auxiliary gas	1.00 L min^{-1}
	Sample gas	1.377 L min^{-1}
	Additional gas	0.372 L min^{-1}
	Accurate Mass	128.9042
	Mass Range	128.689 ÷ 129.119
	Sample time (mass 129 a.u.)	0.05 sec
	Spray chamber	Cyclonic Peltier (2°C)
	Nebulizer	X type, 400 µL min^{-1}
	Scan Type	EScan
	Sensitivity (direct measurement)	300000 cps (1 ng g^{-1} of In)
IC		
	Column	AS 16 (2 mm x 250 mm)
	Guard Column	AG 16 (2 mm x 50 mm)
	Column Temperature	30 °C
	Flow Speed	350 µL min^{-1}
	Suppressor:	ASRS 300 (2 mm)
	Suppressor current	50 mA
	Injection Volume	5 mL
	Eluent	NaOH 35 mM
	Total Runtime	35 min

Table 2. Recovery and accuracy of $^{129}I^-$ in Arctic (NEEM) snow pit samples compared to ultra pure water (UPW). Recovery results are obtained using the regression line equation from figure 1 (slope: 1967 area / pg g^{-1}; intercept 2500). Standard deviation was obtained from repetition measurements (n = 3) of each sample.

Concentration added	Area $^{129}I^-$ (UPW)	Area $^{129}I^-$ (Arctic)	Recovery
0 pgg^{-1}	2610 ± 287	2700 ± 212	---
1 pgg^{-1}	5465 ± 832	3977 ± 147	80%
10 pgg^{-1}	20785 ± 415	16751 ± 608	77%

Table 3. Sample description and their integrated area. < 0.7 pg g^{-1} means below the detection limit.

Sample code	Depth Range (cm from top)	Integrated area	Estimated concentration
Winter 2010	159 – 181	2621	< 0.7 pg g^{-1}
Summer 2010	139 – 158	2425	< 0.7 pg g^{-1}
Winter 2011	82 - 92	2849	< 0.7 pg g^{-1}
Spring 2011	72 - 82	4650	1.2 ± 0.2 pg g^{-1}
Summer 2011	72 - 62	2653	< 0.7 pg g^{-1}
Spring 2012	22 - 27	2896	< 0.7 pg g^{-1}